Cerebral Cortex, November 2016;26: 4253–4264

doi: 10.1093/cercor/bhw263
Advance Access Publication Date: 9 September 2016
Original Article

ORIGINAL ARTICLE

L-DOPA Oppositely Regulates Synaptic Strength and Spine Morphology in D1 and D2 Striatal Projection Neurons in Dyskinesia

Luz M Suarez[1,2], Oscar Solis[1,2], Carolina Aguado[3], Rafael Lujan[3], and Rosario Moratalla[1,2]

[1]Instituto Cajal, Consejo Superior de Investigaciones Científicas, CSIC, 28002 Madrid, Spain, [2]CIBERNED, Instituto de Salud Carlos III, 28002 Madrid, Spain, and [3]Instituto de Investigación en Discapacidades Neurológicas (IDINE), Dept. Ciencias Medicas, Facultad de Medicina, Universidad de Castilla-La Mancha, Campus Biosanitario, Albacete, Spain, Spain.

Address correspondence to Rosario Moratalla, Cajal Institute (CSIC), Av Dr. Arce 37, 28002 Madrid, Spain. Email: moratalla@cajal.csic.es

Abstract

Dopamine depletion in Parkinson's disease (PD) produces dendritic spine loss in striatal medium spiny neurons (MSNs) and increases their excitability. However, the synaptic changes that occur in MSNs in PD, in particular those induced by chronic L-3,4-dihydroxyphenylalanine (L-DOPA) treatment, are still poorly understood. We exposed BAC-transgenic D1-tomato and D2-eGFP mice to PD and dyskinesia model paradigms, enabling cell type-specific assessment of changes in synaptic physiology and morphology. The distinct fluorescence markers allowed us to identify D1 and D2 MSNs for analysis using intracellular sharp electrode recordings, electron microscopy, and 3D reconstructions with single-cell Lucifer Yellow injections. Dopamine depletion induced spine pruning in both types of MSNs, affecting mushroom and thin spines equally. Dopamine depletion also increased firing rate in both D1- and D2-MSNs, but reduced evoked-EPSP amplitude selectively in D2-MSNs. L-DOPA treatment that produced dyskinesia differentially affected synaptic properties in D1- and D2-MSNs. In D1-MSNs, spine density remained reduced but the remaining spines were enlarged, with bigger heads and larger postsynaptic densities. These morphological changes were accompanied by facilitation of action potential firing triggered by synaptic inputs. In contrast, although L-DOPA restored the number of spines in D2-MSNs, it resulted in shortened postsynaptic densities. These changes in D2-MSNs correlated with a decrease in synaptic transmission. Our findings indicate that L-DOPA-induced dyskinesia is associated with abnormal spine morphology, modified synaptic transmission, and altered EPSP-spike coupling, with distinct effects in D1- and D2-MSNs.

Key words: L-DOPA-induced dyskinesia, medium-spiny-neurons, neuronal excitability, Parkinson's disease, striatum

Introduction

Parkinson's disease (PD) is a neurodegenerative disorder characterized by rigidity and slowness of movements caused by the loss of dopaminergic neurons in the substantia nigra (SN). The predominant treatment for PD is administration of L-3,4-dihydroxyphenylalanine (L-DOPA) that initially reverses the motor signs of the disease. Over time however, the combination of disease progression and chronic pulsatile L-DOPA administration

produces abnormal involuntary movements known as dyskinesia (Jenner 2008). The motor complications of PD and L-DOPA-induced dyskinesia are largely mediated by the striatum, which is composed predominantly of GABAergic projection neurons called medium spiny neurons (MSNs) (Kawaguchi 1997). MSNs are classified into 2 types based on their axonal projections and expression of dopamine receptors: MSNs that express D1 receptors (D1-MSNs) preferentially project to SN *pars reticulata* and form the "direct" pathway, whereas MSNs that express D2 receptors (D2-MSNs) project to *globus pallidus* and form the "indirect" pathway (Albin et al. 1989).

MSNs receive topographically organized glutamatergic and dopaminergic inputs, with glutamate receptors localized to the heads and dopamine receptors to the necks of the same dendritic spines. This organization confers to dopamine an important role in regulating MSN spine morphology (Bolam et al. 2000; Deutch et al. 2007). This is illustrated by the finding that decreased dopamine levels in models of PD reduce dendritic spines on MSNs (McNeill et al. 1988; Ingham et al. 1989; Stephens et al. 2005; Zaja-Milatovic et al. 2005; Day et al. 2006; Solis et al. 2007; Villalba et al. 2009; Fieblinger et al. 2014; Toy et al. 2014). We have also shown that striatal dopamine depletion causes a loss of spines in both types of MSN that is selectively restored in D2-MSNs following L-DOPA-treatment (Suarez et al. 2014). This occurs despite the fact that dyskinesia is associated with over-activation of D1-MSNs, indicated by aberrant FosB expression and other molecular changes in D1-MSNs in completely denervated striatal areas (Santini et al. 2007; Darmopil et al. 2009; Murer and Moratalla 2011; Feyder et al. 2011; Ruiz-DeDiego et al. 2015; Solis et al. 2015a, 2015b).

Although dopamine denervation increases MSN firing rate (Calabresi et al. 1993; Azdad et al. 2009; Suarez et al. 2014), the specific electrophysiological changes that occur in each type of MSN in PD and after chronic L-DOPA treatment remain to be fully characterized. Additionally, studies in animal models of other disorders, including schizophrenia or drug-addiction, suggest that alterations in striatal synaptic function are mediated by changes not only in the number of dendritic spines, but also in spine morphology (Robinson and Kolb 2004; Lazcano et al. 2015). Dendritic spines are usually classified into three categories based on their morphology: mushroom, thin, and stubby. Mushroom spines are considered "mature" because they have higher postsynaptic density (PSD) content (Harris et al. 1992), density of glutamate receptors, and synaptic strength (Bourne and Harris 2008). Here, we used *drd1*-tgtomato and *drd2*-eGFP BAC-transgenic mice to study the firing rate and synaptic strength of D1- and D2-MSNs in the dorsolateral striatum after striatal 6-OHDA-lesion (parkinsonian mice) plus chronic L-DOPA treatment (dyskinetic mice) compared with sham-lesioned and saline-treated controls. We also examined the possibility that changes in spine morphology after chronic L-DOPA in dyskinetic animals correlate with alterations in MSN synaptic transmission using electron microscopy and single-cell Lucifer Yellow injections to carry out 3D reconstruction of spines.

Methods and Materials

Animals

This study was carried out in male and female 3–4-month-old hemizygous BAC-transgenic mice (D1R-tmt and D2R-eGFP) in C57BL/6 N background. Animals were housed and maintained following the guidelines from European Union Council Directive (86/609/European Economic Community).

Striatal Lesion and L-DOPA Treatment

Lesions and treatments were performed as described in our previous papers (Pavon et al. 2006; Darmopil et al. 2009; Suarez et al. 2014). Briefly, mice received an intrastriatal injection of 6-OHDA (Sigma-Aldrich, Madrid, Spain; parkinsonian group) or vehicle (sham-lesioned group). After 2–3 weeks, mice were treated with daily intraperitoneal injections of L-DOPA (25 mg/kg; Sigma-Aldrich) preceded by 10 mg/kg benserazide hydrochloride (Sigma-Aldrich; dyskinetic group) or 2 daily saline injections for 14 days. A subgroup of sham-lesioned mice was treated with L-DOPA to use it as control for the L-DOPA effect on lesioned animals. Mice were sacrificed 1 h after the last L-DOPA or saline injection (Supplementary Fig. 1).

Single-Cell Microinjection with Lucifer Yellow and 3D Spine Analysis

Anesthetized mice were perfused transcardially with 4% paraformaldehyde. Brains were postfixed in the same solution for 24 h, and coronal sections (30 and 200 μm thick) were obtained using a vibratome (Leica, Germany). To verify dopaminergic depletion and L-DOPA-induced FosB expression, thinner sections were used for TH (1:1000; Chemicon, Temecula, California) and FosB (1:7500; Santa Cruz Biotechnology, California) immunostaining as previously published (Suarez et al. 2014; data not shown). Adjacent 200 μm sections were used for Lucifer-Yellow injections and spine reconstruction. Fluorescent D1- and D2-MSNs were filled with Lucifer-Yellow (Sigma) as described previously (Suarez et al. 2014) and mounted with prolong®Gold (Invitrogen, Madrid, Spain) for confocal microscopy. Sections were imaged at high magnification (×63 oil) and consecutive z-stacks (z-step of 0.13 μm) were acquired with a Leica SP-5 confocal microscope. For each stack of images, confocal parameters were set so that fluorescence signal was as bright as possible while ensuring that there were no pixels saturated within the spines. Images were deconvolved using LAS AF 2.5 software (Leica, Germany), and spine analysis was performed using the semiautomated software NeuronStudio (http://research.mssm.edu/cnic/tools-ns.html). NeuronStudio analyzes spines in 3D and classifies them into 3 major morphologic types (mushroom, thin, and stubby) based on spine head diameter and presence/absence of a discernible spine neck (Harris et al. 1992; Rodriguez et al. 2008; Dumitriu et al. 2012). After NeuronStudio processing, all spines were verified and errors were corrected manually by a researcher blinded to experimental conditions. We analyzed 6–8 neurons per animal (Table 1).

Electron Microscopy

Anesthetized mice were perfused with 4% paraformaldehyde, with 0.05% glutaraldehyde and 15% (v/v) picric acid. Brains

Table 1 Numbers of mice and MSNs for spine analysis

Treatment (*n*)	D1R-tmtmice	D1-MSNs analyzed	D2R-eGFP mice	D2-MSNs analyzed
Sham-lesioned saline (15)	8	64	7	58
Sham-lesioned L-DOPA (4)	3	23	2	16
Parkinsonian (14)	7	45	7	50
Dyskinetic (14)	7	54	7	53

were removed and immersed in the same fixative for 2 h or overnight at 4°C. Coronal 60 μm thick sections were cut on a vibratome (Leica). Then we performed immunohistochemistry for EM using the pre-embedding immunogold technique, as previously described (Lujan et al. 1996). Briefly, free-floating sections were incubated with the primary antibodies (anti-tomato, (Clontech, France), or anti-GFP; (Nacalai, Japan) 1–2 μg/ml), and with the appropriate secondary antibody coupled to 1.4 nm gold (Nanoprobes Inc., Stony Brook, NY, USA), followed by silver enhancement of the gold particles with an HQ Silver kit (Nanoprobes Inc.). Next, sections were treated with 1% osmium tetraoxide and block-stained with uranyl acetate, dehydrated, and flat-embedded on glass slides in Durcupan (Fluka) resin. Regions of interest were cut on an ultramicrotome (Reichert Ultracut E, Leica, Austria; 70–90 nm), and then collected on pioloform-coated single slot copper grids. Contrast for EM was performed on drops of 1% aqueous uranyl acetate and Reynolds's lead citrate. Ultrastructural observation and analysis was carried out in a Jeol-1010 electron microscope. Electron photomicrographs were captured with ORIUS SC600B CCD camera (Gatan, Munich, Germany).

To analyze structural changes to the spines, we used 60 μm coronal slices processed for pre-embedding immunogold-immunohistochemistry. Three samples of tissue per animal were obtained for preparation of embedding block. To minimize false negatives, EM serial ultrathin sections were cut close to the surface of each block, always selecting areas with optimal gold labeling (5–10 μm from the surface). Randomly selected areas of each section were captured with a final magnification of ×50 000. All spines establishing synapses with axon terminals containing immunoparticles for tomato or eGFP were counted. The length of the synaptic membrane specialization and the extrasynaptic membrane from all immunopositive spines was measured using a digitizing tablet and appropriate software (Image J). Around 90–120 synapses were analyzed from 6 mice (3 D1R-tmt and 3 D2R-eGFP) in each experimental group.

Electrophysiology Recordings

Anesthetized mice were decapitated and brains were removed and dropped into ice-cold Krebs–Ringer bicarbonate (KRB) solution containing (in mM): 119 NaCl, 26.2 $NaHCO_3$, 2.5 KCl, 1 KH_2PO_4, 1.3 $MgSO_4$, 2.5 $CaCl_2$, and 11 glucose, gassed with 95% O_2 and 5% CO_2. Transverse 350 μm cortico-striatal slices were cut with a vibratome (Leica) and stored for >1 h at room temperature. Recordings were performed in a submersion-type chamber continuously perfused (2 ml/min) with KRB solution at 31–32°C in presence of 100 μm picrotoxin (Sigma) to block GABAA receptors. Glutamatergic responses were evoked at 0.033 Hz with a bipolar-stimulating-electrode located in the white matter. D1- and D2-MSNs located in dorsal striatum were identified by fluorescence using infrared differential interface contrast on an upright DM6000FS Leica microscope. Sharp electrodes for intracellular recording were filled with 2 M KCl (30–60 MΩ). Signals were recorded with an Axoclamp-2B amplifier (Axon Instruments, Foster City, CA, USA) used in bridge mode and stored and analyzed on a digital system (pClamp 10.0, Molecular Devices, CA, USA). Passive and active electrophysiological properties were obtained from the membrane responses of MSNs to current injections in current-clamp mode. More specifically, the input resistance (Rin) of the MSNs was calculated from the voltage deflection produced by hyperpolarizing current pulses (0.1–0.4 nA) of 500 ms duration. To extract properties of the action potentials (APs), we used 200 ms depolarizing current pulses of increasing amplitude (0.1 nA) obtained of 3 consecutive sweeps (0.066 Hz). AP parameters were measured in the first AP of a burst. The AP threshold was measured as the potential at which dV/dt first exceeds 10 V/s (Stuart et al. 1997). The AP amplitude was measured as the difference between the membrane potential immediately before the current pulse and the maximum amplitude value attained by the AP. The after-hyperpolarization (AHP) amplitude was calculated from the voltage deflection produced after AP averaging 3–4 consecutive responses. For EPSP-induced action potential, we measured the AP threshold of 2 consecutive sweeps evoked at a frequency of 0.066 Hz. The changes in threshold of the EPSP-spike were determined in relation with the RMP. Firing rate was determined by injecting depolarized-current-steps (200 ms) through a sharp electrode and measuring the resulting spiking. We recorded from 1 or 2 neurons per slice (Table 2).

Statistical Analysis

Data are reported as average ± S.E.M. or box and whisker plots showing median, quartiles and ranges. Statistical evaluations and graphs were performed using SigmaPlot 12.0 (Systat-Software Inc. San Jose, CA, USA). Statistical differences were assessed by one-way ANOVA followed by Bonferroni post hoc test or Kruskal–Wallis analysis followed by Dunn´s test for not parametric data. A value of $P < 0.05$ was considered statistically significant.

Results

DA Depletion Increases Excitability of D1-MSNs

As we previously demonstrated (Suárez et al. 2014), spine density was dramatically reduced in D1-MSNs in completely dopamine denervated striatal areas (Fig. 1A). To test whether this spine reduction was accompanied by altered intrinsic excitability, we injected depolarizing steps of current through a recording electrode positioned in the soma of identified D1-MSNs. The same depolarizing current evoked significantly more action potentials in D1-MSNs in 6-OHDA mice compared with sham-lesioned mice (Fig. 1B), indicating a rise in the firing rate in the parkinsonian model. While the resting membrane potential (RMP) and input resistance (R_{in}) were unchanged in parkinsonian mice (Table 3), the action potential threshold was lower compared with sham-lesioned animals (–53.5 ± 2.7 vs. –46.8 ± 0.5 mV; $P < 0.05$, Table 1). Moreover, there was a nonsignificant reduction of the minimal current necessary to generate action potentials or rheobase in 6-OHDA-lesioned mice compared with sham-lesioned (Table 3). These data are consistent with the hypothesis that in 6-OHDA animals, D1-MSNs scale up their firing rates in response to the decreased synaptic excitation caused by spine loss (Calabresi et al. 1993; Azdad et al. 2009).

To test this idea further, we examined if there were changes in the stimulus–response curve in this model. In the presence of picrotoxin (a $GABA_A$ antagonist) to avoid contamination by IPSPs, we found no distinguishable differences in EPSP amplitude

Table 2 Numbers of mice and MSNs for electrophysiological analysis

Treatment (*n*)	D1R-tmtmice	D1-MSNs analyzed	D2R-eGFP mice	D2-MSNs analyzed
Sham-lesioned (18)	8	9	10	10
Parkinsonian (18)	10	12	8	12
Dyskinetic (23)	11	12	12	14

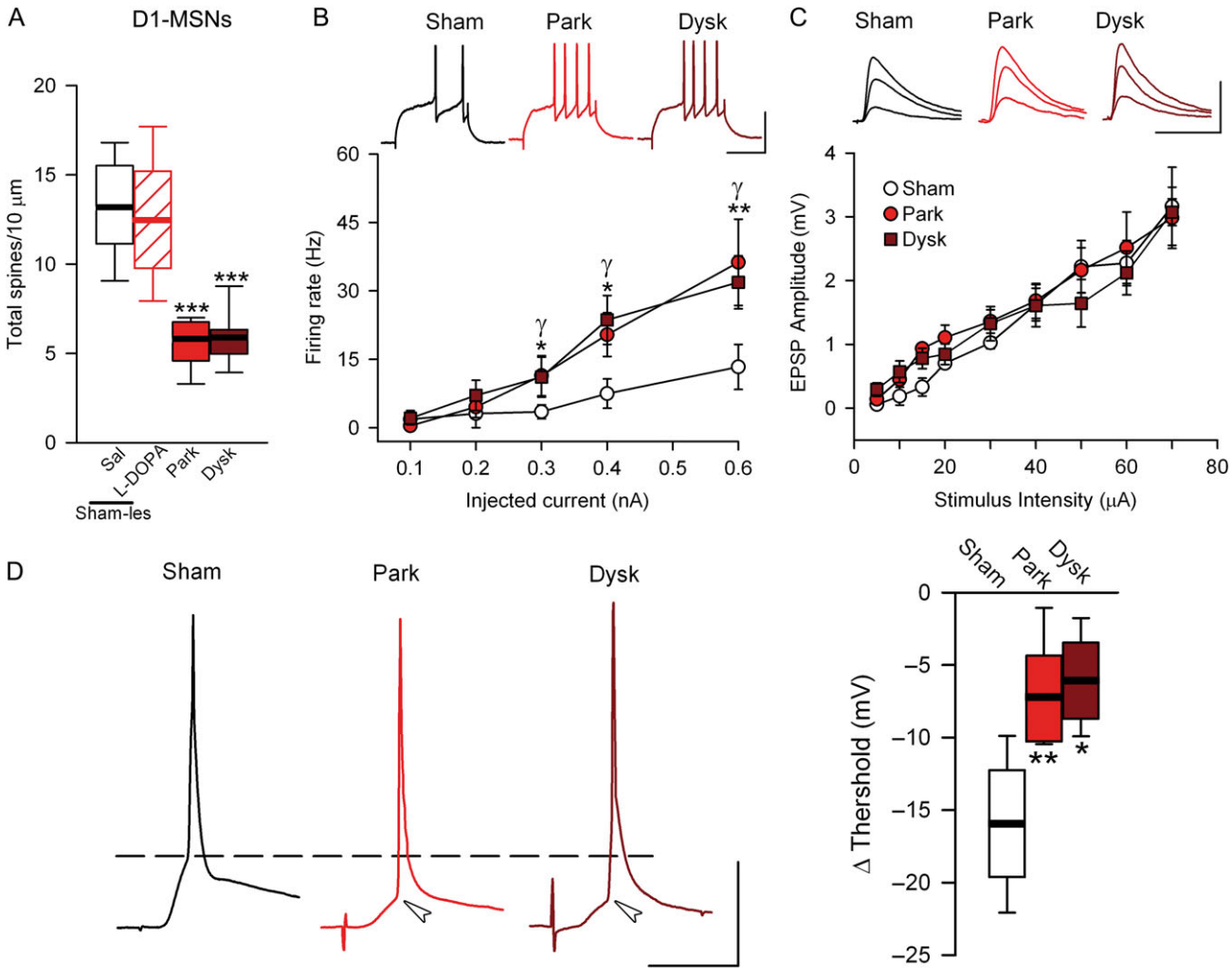

Figure 1. Synaptic transmission and neural excitability are altered in PD and dyskinesia in direct striatal projection neurons. (*A*) Number of dendritic spines in 10 µm of D1-MSNs. (*B*) Number of action potential (AP) as a function of injected current intensity in D1-MSNs. Top, representative examples of firing rate at 0.4 nA of injected current. Scale bar = 50 mV/50ms. (*C*) Evoked-EPSP amplitude values across stimulus intensity in D1-MSNs. Top, representative examples of evoked EPSPs at 20, 40, and 60 µA. Scale bar 10 mV/20ms. (*D*) Illustrative traces of APs evoked by synaptic stimulation in each experimental condition in D1-MSNs (left) Summary of changes in the threshold of synaptically evoked APs; (*$\gamma P < 0.05$, **$\gamma\gamma P < 0.005$ parkinsoninan or dyskinetic mice respectively vs. sham-lesioned; one-way ANOVA).

Table 3 Intrinsic membrane properties of MSNs. Data presented as mean ± SEM. The number of MSNs-recorded in each condition is expressed in parentheses following the condition. *P < 0.05; **P < 0.01 vs. sham-lesioned

	D1-MSNs			D2-MSNs		
	Sham (7)	Park (8)	Dysk (13)	Sham (9)	Park (8)	Dysk (11)
Passive membrane properties						
RMP (mV)	−83.8 ± 3.9	−83.8 ± 2.5	−85.5 ± 3.1	−88.2 ± 2.6	−89.5 ± 2.3	−88.7 ± 1.7
Rin (mΩ)	42.8 ± 5.4	45.6 ± 4.3	46.0 ± 3.7	46.8 ± 3.8	47.6 ± 0.5	48.4 ± 5.7
Active membrane properties						
AP						
Threshold (mV)	−46.8 ± 0.5	−53.5 ± 2.7*	−51.1 ± 2.1	−48.8 ± 2.3	−48.9 ± 1.7	−49.3 ± 2.8
Amplitude (mV)	88.2 ± 7.3	76.2 ± 5.6	88.6 ± 5.4	87.0 ± 5.3	85.4 ± 10.3	91.1 ± 6.4
Width (ms)	0.76 ± 0.07	0.91 ± 1.01	0.89 ± 0.08	0.76 ± 0.07	0.89 ± 0.02	0.82 ± 0.08
AHP Amplitude (mV)	−4.9 ± 1.2	−7.5 ± 0.9	−6.9 ± 1.3	−4.6 ± 0.9	−5.1 ± 0.5	−8.6 ± 0.9
Rheobase (nA)	0.46 ± 0.06	0.33 ± 0.05	0.29 ± 0.04*	0.46 ± 0.05	0.24 ± 0.03**	0.29 ± 0.03*

between sham-lesioned and parkinsonian mice at any stimulus intensity tested (Fig. 1C). These results indicate that the stimulus–response curve was not altered by dopamine depletion. In addition, presynaptic glutamate release, measured by paired-pulse ratio (PPR), did not change after the lesion (Supplementary Fig. 2A). We then tested if synaptic transmission facilitates firing in D1-MSNs in 6-OHDA-lesioned mice by increasing the stimulus intensity to trigger an action potential by an evoked-EPSP. We

found a significant decrease in the threshold for evoked action potentials in parkinsonian compared with sham-lesioned mice (Fig. 1D; Supplementary Table 1).

A reduction in the complexity of the dendritic tree could compensate for the loss of spines and contribute to the maintenance of synaptic strength. We therefore next analyzed the length and number of branches and primary dendrites of the dendritic tree of D1-MSNs in parkinsonian mice. Consistent with our previous report (Suarez et al. 2014), the complexity of the dendritic tree did not change after 6-OHDA lesion (Supplementary Fig. 3A). Chronic L-DOPA treatment in dyskinetic animals did not significantly alter the electrophysiological changes or the spine density observed in D1-MSNs in parkinsonian mice (Fig. 1A–D). In sham-lesioned mice, L-DOPA does not modify the spine density (Fig. 1A) or dendritic tree complex (Supplementary Fig. 3).

L-DOPA Treatment Restores Spine Density and Excitability in D2-MSNs

In D2-MSNs, spine density was reduced after 6-OHDA-lesion (Fig. 2A), as reported previously (Day et al. 2006; Fieblinger et al. 2014; Suarez et al. 2014). As expected, the firing rate was increased (Fig. 2B) after 6-OHDA. In contrast, no changes in passive membrane properties or action potential threshold were found in D2-MSNs from parkinsonian mice, although the rheobase was decreased compared with sham-lesioned animals (Table 3). In addition, the stimulus–response curve was shifted downward in D2-MSNs across all stimulus intensities tested (Fig. 2C). In these cells, we did not observe any significant change in the threshold for synaptically evoked action potentials (Fig. 2D; supplementary Table 1). Similar to the results in D1-MSNs, 6-OHDA-lesions did not change PPR or dendritic tree complexity in D2-MSNs (supplementary Figures 2B, 3B).

Chronic L-DOPA treatment restored spine density in D2-MSNs during peak-dose dyskinesia states (Fig. 2A) as previously reported (Suarez et al. 2014). L-DOPA also restored the intrinsic excitability and the firing rate of D2-MSNs at lower intensities, although the excitability remained elevated at higher intensities (Fig. 2B). Moreover, the rheobase remained decreased in dyskinetic mice compared with sham-lesioned mice (0.29 nA vs. 0.46 nA; $P < 0.05$; Table 3). However, in dyskinetic mice the stimulus–response curve was shifted downward at all stimulus

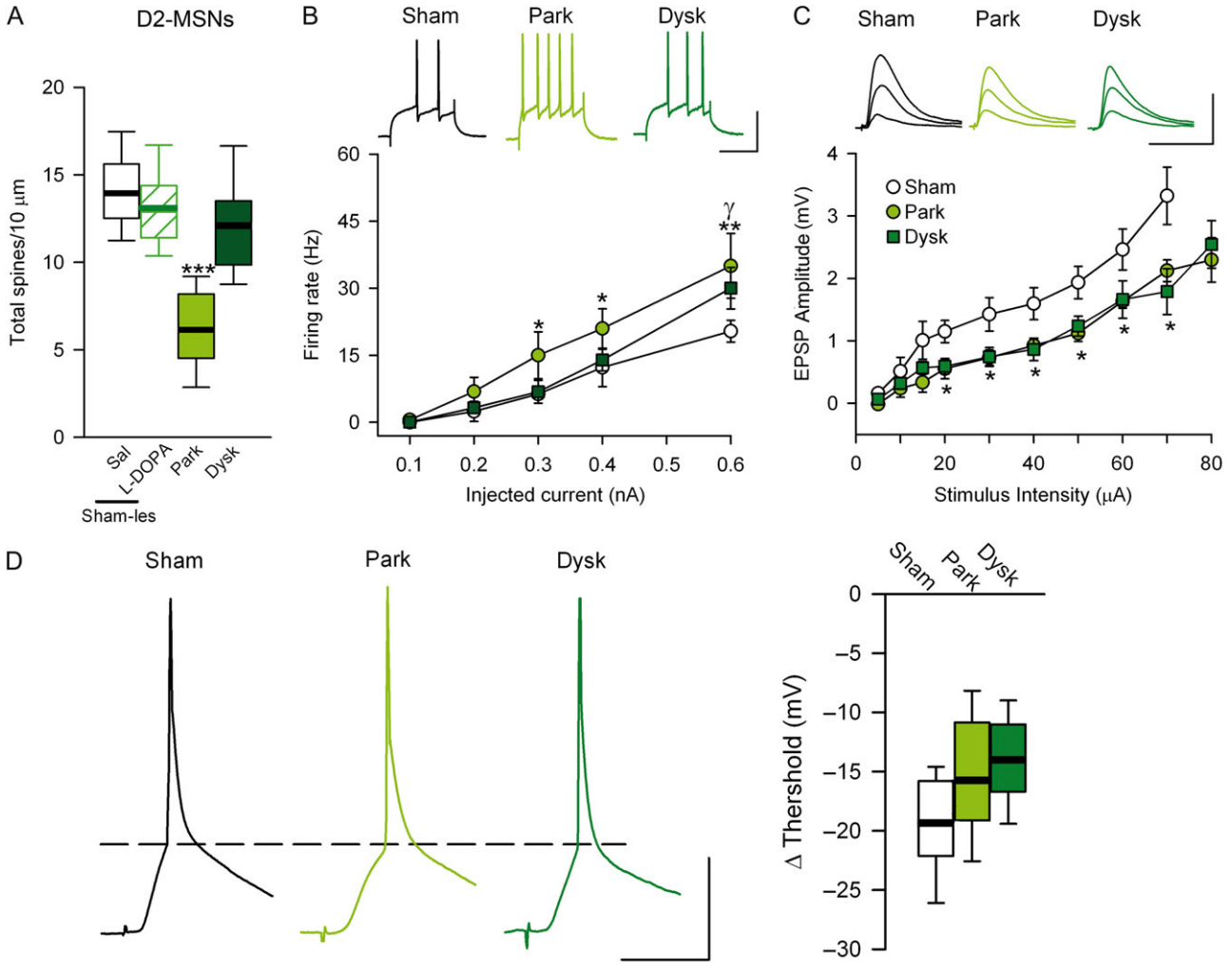

Figure 2. Synaptic transmission and neural excitability are altered in PD and dyskinesia in indirect striatal projection neurons. (*A*) Spine density (number of spines in 10 µm) in D2-MSNs. (*B*) Firing rate of D2-MSNs. Top, representative firing rate at 0.4 nA of injected current. Scale bar = 50 mV/50ms. (*C*) Synaptic transmission of D2-MSNs remains decreased in dyskinetic mice. Top, representative EPSP-stimulus intensity at 20, 40 and 60 µA. Scale bar = 10 mV/20ms. (*D*) Illustrative traces of APs evoked by synaptic stimulation in each experimental condition in D2-MSNs (left). Summary of changes in the threshold of synaptically evoked APs (right). (*γ$P < 0.05$, **γγ $P < 0.005$ parkinsoninan or dyskinetic mice respectively vs. sham-lesioned; one-way ANOVA).

intensities tested compared with sham-lesioned mice (Fig. 2C). Furthermore, the threshold for synaptic stimulation-evoked action potentials did not change in dyskinetic compared with sham-lesioned mice (Fig. 2D, Supplementary Table 1). These data suggest that the new spines formed in response to L-DOPA treatment in parkinsonian mice may not be completely functional. In sham-lesioned mice, L-DOPA treatment did not produce any changes in spine density (Fig. 2A) or dendritic tree (Supplementary Fig. 3B).

PSD Length is Increased in D1—But Reduced in D2-MSN Spines After L-DOPA

Since dendritic spine morphology partly determines synaptic strength (Yuste and Bonhoeffer 2004; Bourne and Harris 2008), we sought to determine if changes observed in afferent drive of spike firing in D1- and D2-MSNs from parkinsonian and dyskinetic mice were due to changes in the size of spines. Using EM, we found that the length of the remaining dendritic spines in D1-MSNs is similar in parkinsonian and sham-lesioned mice (Fig. 3A). However, chronic L-DOPA treatment in lesioned mice increased the total length of dendritic spines compared with both sham-lesioned and parkinsonian mice (1911 ± 126 vs. 1571 ± 11 and 1516 ± 74 nm, respectively; Fig. 3A). These results suggested that dendritic spines in D1-MSNs are closer to presynaptic terminals in dyskinetic mice. In order to form functional synapses, postsynaptic receptors must be anchored to the postsynaptic membrane via binding to membrane-associated scaffolding proteins such as PSD-95. Therefore, we used EM to analyze PSD length in MSN spines. We observed a significant increase in PSD-length in D1-MSNs in dyskinetic mice compared with sham-lesioned and parkinsonian animals (Fig. 3B,C). Concerning D2-MSNs, dopamine depletion did not change spine length or PSD length compared with sham-lesioned animals (Fig. 3D,E). While L-DOPA-induced dyskinesia was not accompanied by changes in spine length in D2-MSNs, but there was a decrease in PSD length compared with sham-lesioned and parkinsonian mice (206.51 ± 3.92 vs. 261.16 ± 6.94 and vs. 258.67 ± 7.25 nm, respectively; Fig. 3E,F).

Restoration of Spines in D2-MSNs of Dyskinetic Mice Occurs Uniformly Across Spine Subtypes

We first quantified each subtype of spines in D1- and D2-MSNs using the semiautomated software NeuronStudio. Both types of striatal projection neurons have mushroom, thin, and stubby spines (Fig. 4A–D), although mushroom and thin spines were more abundant than stubby spines in the normal striatum. L-DOPA treatment did not alter the proportion of spine subtypes in sham-lesioned mice (Fig. 5A,C). Because changes in the proportion of spine subtypes have been shown to influence synaptic transmission and plasticity (Bourne and Harris 2008), we studied whether the changes observed in synaptic transmission and PSD length in PD and dyskinesia were due to changes in the relative number of spine types. Dopamine depletion reduced spine density similarly (around 50%) in both immature (thin) and mature (mushroom) spines in D1- and D2-MSN (Fig. 5A–D). L-DOPA treatment in dyskinetic animals did not alter spine loss or the proportion of spine subtypes in D1-MSNs (Fig. 5A,B), but produced a recovery in the number of both mushroom and thin spines in D2-MSNs (Fig. 5C,D). There was a small increase in the number of stubby spines in D2-MSNs in parkinsonian mice (Fig. 5C). Because spine size has been shown to be correlated with synaptic strength (Bourne and Harris 2008), we next studied the effect of parkinsonism and dyskinesia on the volume and length of mushroom and thin spines. We also measured the head and neck diameter of mushroom spines because they have larger PSDs compared with the other spine types and form “mature” synapses (Harris et al. 1992). Dopamine depletion did not change the volume or the length of mushroom and thin spines in D1-MSNs (Fig. 6A), but increased the neck diameter of mushroom spines. Compared with sham-lesioned animals, L-DOPA treatment in dyskinetic animals increased the volume and length of mushroom spines in D1-MSNs. These increases correlated with an increase in the diameter of spine heads and a widening of the neck diameter (Fig. 6A). In D2-MSNs, dopamine depletion decreased the length of thin spines by about 15%, which was reversed by L-DOPA

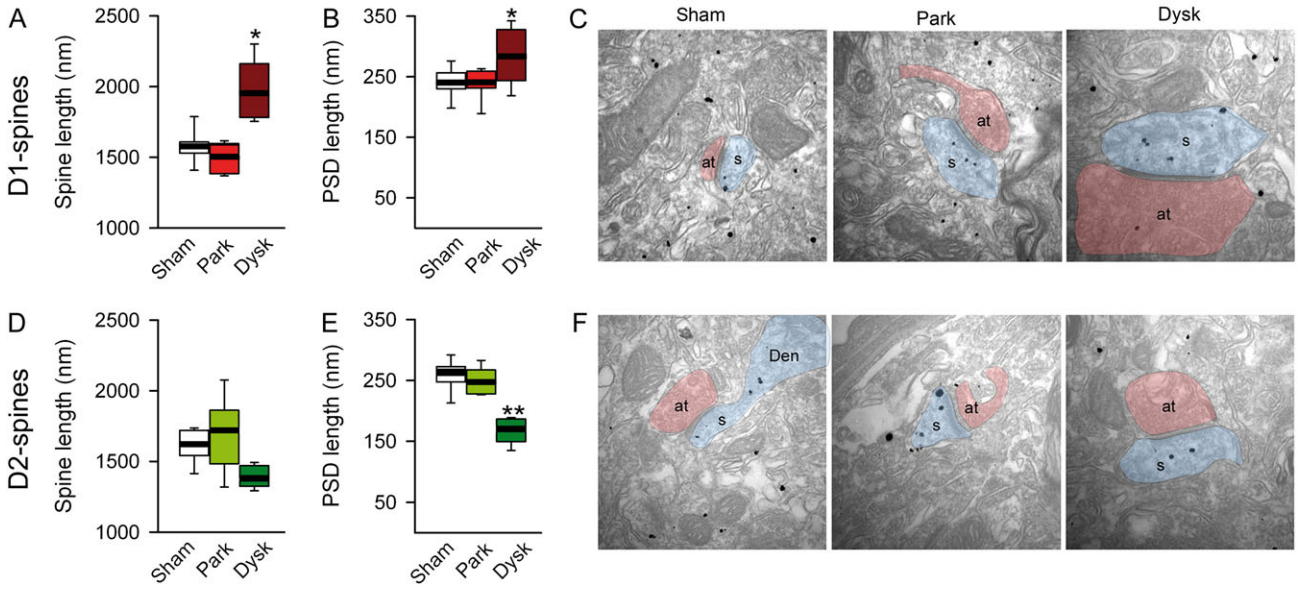

Figure 3. PSD length is decreased in D2-MSNs in dyskinesia. EM analysis of spine length (A) and PSD length (B) in D1-MSNs. (C) Representative images of spines from D1-MSNs in each experimental condition. Spine length (D) and PSD length (E) of D2-MSNs. (F) Representative EM illustration of spine from D2-MSNs (*P < 0.05, **P < 0.005 vs. sham-lesioned; one-way ANOVA). at: axon terminal; s: spine.

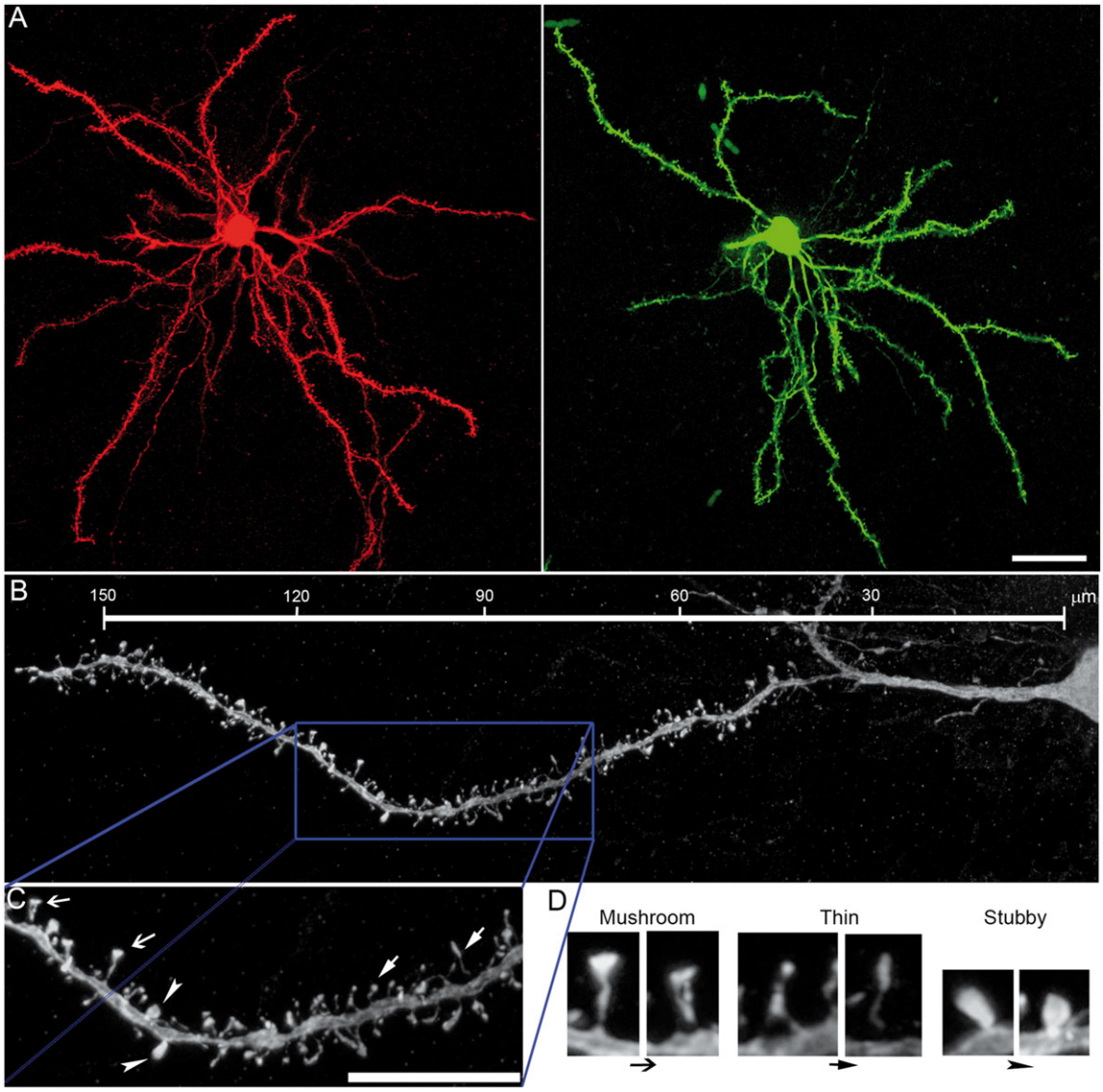

Figure 4. 3D morphometric analysis of types of spines in D1- and D2-MSNs. (*A*) Complete morphological reconstruction of D1-MSNs (red) and D2-MSNs (green). Scale bar = 25 µm. (*B*) Confocal image of a complete dendrite and high magnification (*C*) of a selected area in B (blue box) illustrating the types of spines quantified. Scale bar = 15 µm. (*D*) Higher magnification of spines indicated by arrows in C. Scale bar = 0.5 µm.

treatment (Fig. 6*B*). The neck diameter of mushroom spines in D2-MSNs was also decreased in dyskinetic mice (Fig. 6*B*).

Discussion

Our results indicate that in parkinsonian mice both D1- and D2-MSNs lose the major types of striatal spines—mushroom and thin—and become more excitable. This loss of spines is accompanied by a decrease in synaptic strength in D2-MSNs, but not in D1-MSNs, in which we observed facilitation of synaptic transmission. In dyskinetic mice, spine density and firing rate recovered selectively in D2-MSNs, but synaptic strength remained decreased and the newly formed spines had lower PSD-content. These results suggest that the new spines are weaker. By contrast, in D1-MSNs there was no recovery in spine number or firing rate, but the remaining spines were enlarged, with bigger head and neck diameters, which likely contributed to the maintenance of synaptic strength.

Intrinsic Excitability Increases in PD in Both D1- and D2-MSNs

Previous studies showed that striatal denervation enhances MSN membrane excitability (Calabresi et al. 1993; Azdad et al. 2009; Suarez et al. 2014) but did not examine whether this increase occurs in one or in both types of projection neurons. Here, we demonstrated that both MSN types display enhanced firing rates after 6-OHDA-lesion. In D1-MSNs, both the action potential threshold and the rheobase were decreased, whereas in D2-MSNs only rheobase was decreased. Dopamine release has opposite effects on the firing rate of striatal projection neurons: D1-receptor activation increases spiking in D1-MSNs, while D2-receptor activation decreases it in D2-MSNs (Gerfen and Surmeier 2011). Thus, it would be expected that loss of dopamine in 6-OHDA-lesioned mice decreases firing in D1-MSNs but increases it in D2-MSNs. However, we found that in parkinsonian mice, D1-MSNs increased their firing rate, as previously

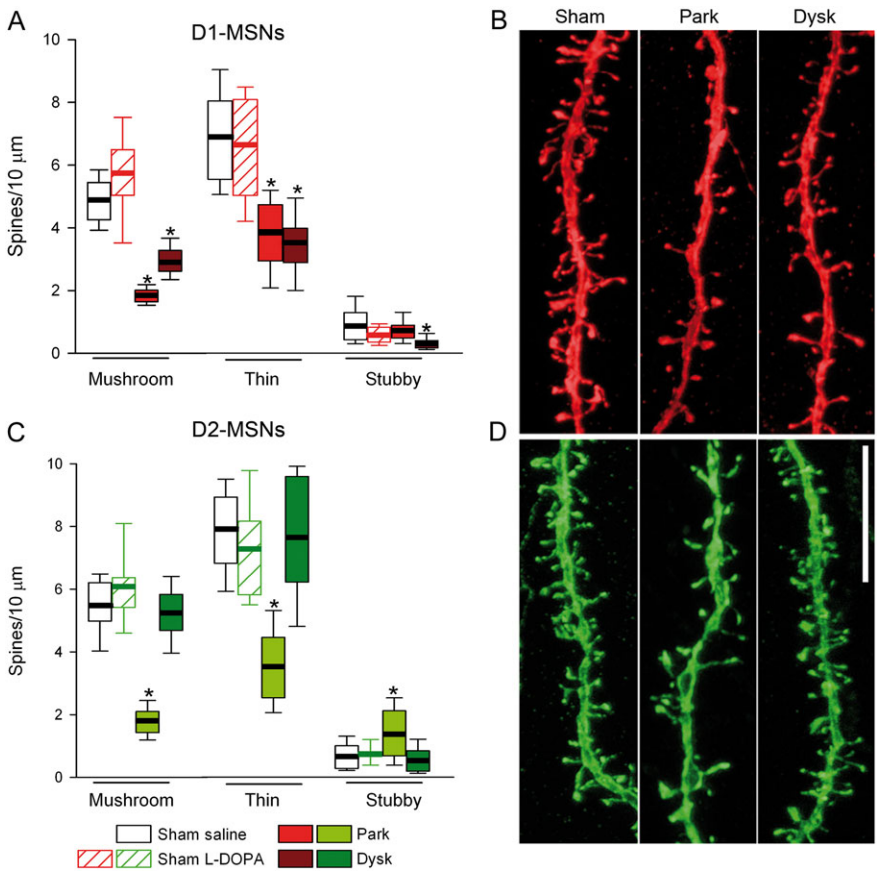

Figure 5. Effects of DA depletion and L-DOPA treatment on the proportion of dendritic spine types in identified MSNs. (*A*) Number of mushroom, thin, and stubby spines per 10 µm in D1-MSN dendrites. (*B*) Representative confocal images of D1-MSN dendrites. (*C*) Quantification of the types of dendritic spines in D2-MSNs. (*D*) Illustrative confocal images of D2-MSNs; Scale bar 10 µm (*$P < 0.05$ vs. sham-lesioned; Kruskal–Wallis test).

reported (Fieblinger et al. 2014). This apparently paradoxical finding can be explained by previous reports that D1-receptor activation exerts multiple actions over D1-MSN excitability. It facilitates spiking by enhancing currents through L-type Ca^{2+} channels and decreasing K^+ currents (Surmeier et al. 1995; Galarraga et al. 1997). However, D1-receptor activation also reduces excitability by decreasing the conductance of somatic voltage-gated Na^+ channels (Gerfen and Surmeier 2011) and decreasing the conductances of dendritic Ca^{2+} channels (P- and N-types) (Westenbroek et al. 1992; Usowicz et al. 1992; Calabresi et al. 1999; Calabresi et al. 2000). Here, we observed facilitation of EPSP-spike coupling in parkinsonian mice due to the decreased threshold for action potential firing, suggesting that lack of dopamine might release somatic Na^+ channels from the control of D1-receptor activation. Another possibility is that this might occur through changes in striatal microcircuit, perhaps by recruiting cholinergic interneurons. This is consistent with the previous report that nicotine alleviates neuronal hyperexcitability in parkinsonian rats (Plata et al. 2013; Pérez-Ortega et al. 2016), whereas cholinergic M4-receptors increase the excitability of D1-MSNs but not of D2-MSNs (Hernandez-Flores et al. 2015). The excitability of D2-MSNs is modulated by D2-receptor activation, which causes decreases in Ca^{2+} conductance and increases in K^+ conductance, pushing neurons to a less excitable state (Gerfen and Surmeier 2011). Accordingly, the loss of dopamine should increase the excitability of D2-MSNs. Indeed, while D2-MSNs in parkinsonian mice were more likely to fire to an action potential in response to direct depolarization of the soma, they were less likely to fire in response to EPSPs, and therefore less excitable.

However, in dyskinetic animals, there is an imbalance between direct and indirect striatal projection neurons, whereas hyper-excitability persists in D1-MSNs, it returns to normal in D2-MSNs after L-DOPA treatment. These opposite effects of L-DOPA on firing rate might contribute to the postulated functional imbalance favoring the direct over the indirect pathway in dyskinesia models.

Synaptic Morphology Changes in PD

Our results show that in the healthy dorsal striatum, mushroom and thin spines predominate in both D1- and D2-MSNs, in line with results in the nucleus accumbens (Dumitriu et al. 2012). Furthermore, we showed that dopamine depletion reduces the density of immature (thin) and mature (mushroom) spines similarly in both MSN types, although increases stubby spines in D2-MSNs, presumably due to the mushroom spines that became stubby-like before their disappearance. Because mushroom spines contain more glutamate receptors (Bourne and Harris 2008), we expected that loss of mushroom spines would lead to reduced cortico-striatal transmission is diminished in both striatal output circuits in parkinsonian mice. However, we found that stimulus–response curve decreased only in D2-MSNs, suggesting that mechanisms specific to D1-MSNs compensate for the decrease in spine number. Compensation could occur through an increase in the AMPA:

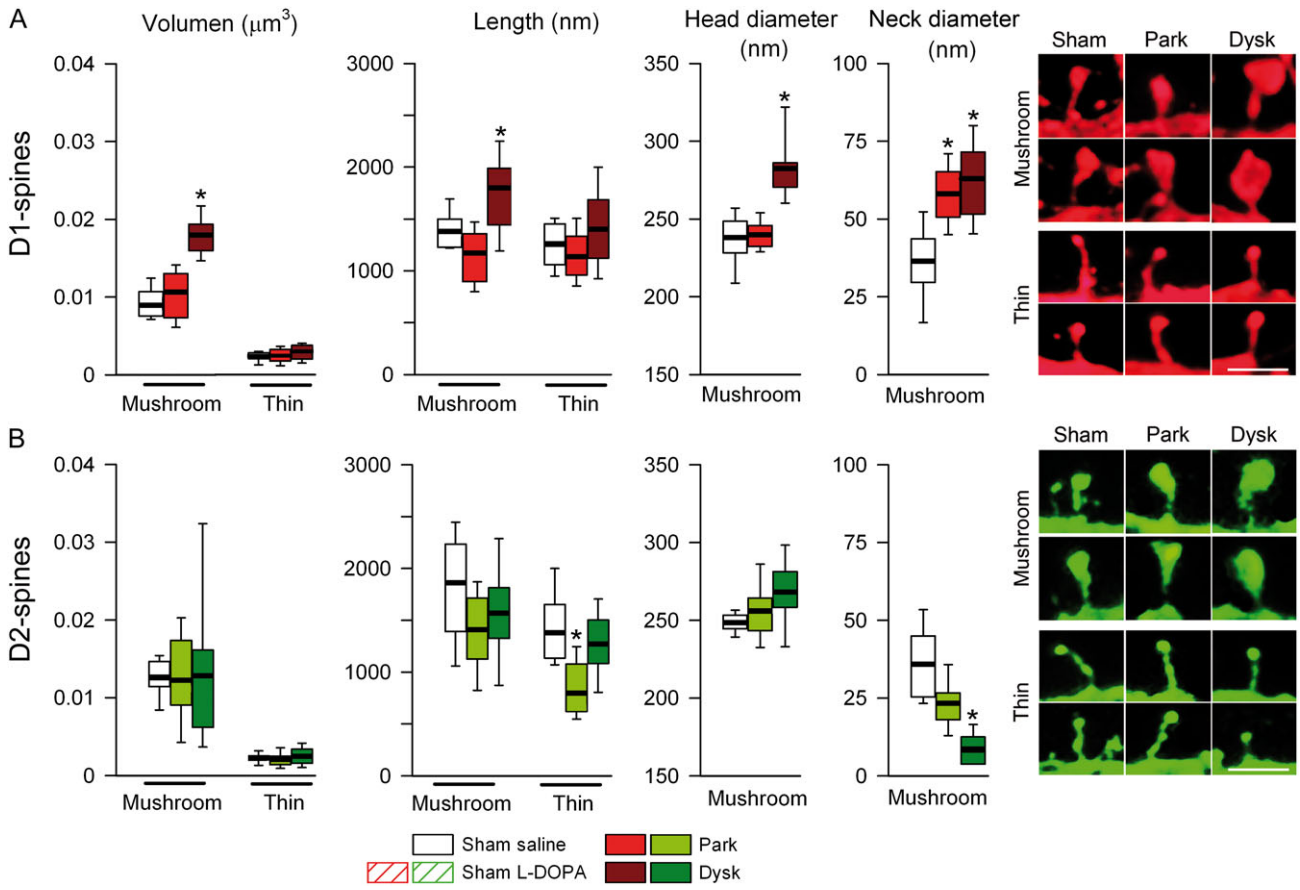

Figure 6. Morphology of mushroom spines is modified selectively in D1-MSNs in dyskinetic mice. (*A*) Quantification of volume and length of mushroom and thin spines and head and neck diameter of mushroom spines of D1-MSNs. *Right*: Representative high magnification of mushroom (top) and thin (bottom) spines from D1-MSNs. Scale bar = 0.75 μm. (*B*) Analysis of the dendritic spines in D2-MSNs. *Right*: Representative mushroom (top) and thin (bottom) spines from D2-MSNs. Scale bar = 0.75 μm (*$P < 0.05$ vs. sham-lesioned; Kruskal–Wallis test).

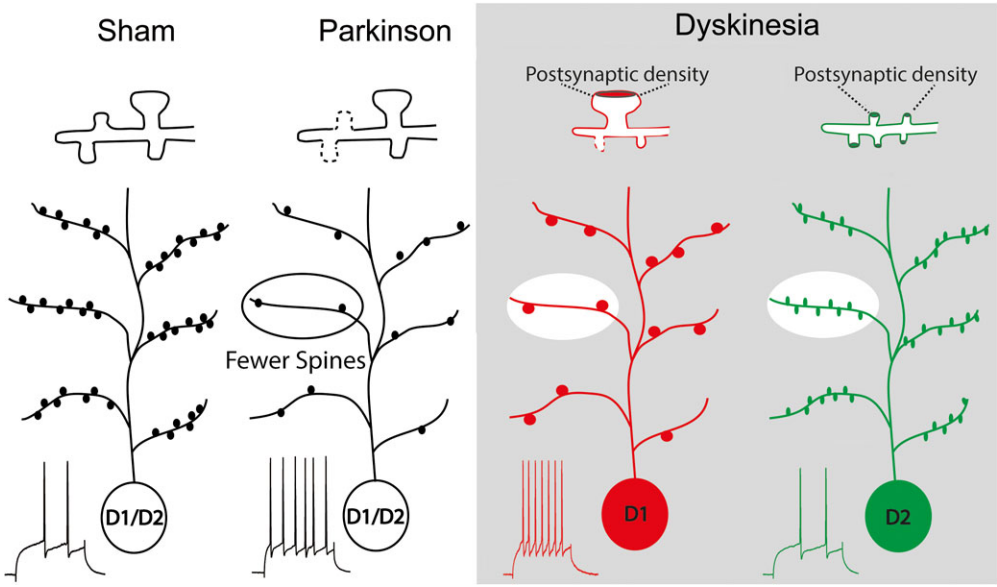

Figure 7. Schematic representation of the synaptic pathology described in PD and dyskinesia for D1- and D2-MSN. In sham-lesioned mice, both MSN types have similar spine density and excitability (as measured by action potential). In PD, both MSN types undergo pruning of spines and scale up firing rate. In dyskinetic mice, the enlarged remaining spines in D1-MSNs, with larger PSDs (inset), may explain the observed maintenance of synaptic transmission. In contrast, in D2-MSNs, spine number recovers, but the weaker new spines are insufficient to recover the loss of synaptic weight.

NMDA ratio, which is selectively increased in D1-MSNs after 6-OHDA lesion (Parker et al. 2016). Another possibility, in light of the fact that dendritic arborization does not change, is that the increased neck diameter of mushroom spines on D1-MSNs allows higher Ca^{2+} influx after dopamine denervation as shown by Plata et al. (2013), thus maintaining synaptic strength despite spine loss. We cannot exclude the possibility that only the cortico-striatal "dumb" or silent spines (which do not form functional synapses) are lost following dopamine denervation, as previously has been reported (Toy et al. 2014; Villalba et al. 2014). In contrast, in parkinsonian mice, there was no change in D2-MSN spine morphology (spine and PSD length), thus synaptic transmission decreased in concordance with spine loss.

Aberrant Synaptic Remodeling in Dyskinesia

Consistent with our previous results (Suarez et al. 2014), we now show that L-DOPA does not restore the spine loss observed in D1-MSNs following 6-OHDA lesion, but normal synaptic strength is maintained. Interestingly, the remaining spines are enlarged, with wider necks and bigger heads. In hippocampal neurons, similar changes in spine volume correlate with larger glutamatergic synaptic areas and higher synaptic strength (Bourne and Harris 2008). Thus, the changes we observed in D1-MSN spine volume and PSD length may explain how synaptic weight is maintained despite spine loss. This is consistent with previous results showing an increased interaction between D1R and PSD95 after L-DOPA (Porras et al. 2012), and an increased number of cortical inputs to MSNs (Zhang et al. 2013), that specifically potentiates the response to glutamate in D1-MSNs in dyskinetic animals (Gardoni et al. 2006; Andre et al. 2010). It is possible that these changes are related to FosB overexpression, as previous results demonstrate that FosB overexpression decreases the number of silent synapses in the ventral striatum (Grueter et al. 2013).

By contrast, in D2-MSNs we observed the opposite: L-DOPA restored normal spine density, as shown previously (Fieblinger et al. 2014; Suarez et al. 2014), but synaptic strength remained decreased. As discussed above for the D1-MSNs, this may be explained by changes in Ca^{2+} entry, since the neck diameters of the newly born D2-MSN spines are thinner, presumably resulting in decreased synaptic Ca^{2+} currents. In addition, the spines of D2-MSNs in dyskinetic mice have smaller PSDs, and thus possibly fewer glutamate receptors, a correlation demonstrated in hippocampal neurons (Yuste and Bonhoeffer 2004). Another possibility is that L-DOPA increases spine turnover in D2-MSNs preventing their maturation.

Our findings provide the first evidence that altered spine morphology in dyskinetic animals indicates aberrant cortico-striatal physiology, contributing to the motor symptoms observed in dyskinesia. This is consistent with findings in other brain regions, where spine morphology has been shown to be a critical determinant of the strength and plasticity of glutamatergic transmission (Bourne and Harris 2008). A remaining issue for future experiments is whether pharmacological manipulations that alleviate dyskinetic symptoms such as amantadine or nicotine (Plata et al. 2013) further modify this structural and synaptic plasticity.

In summary, we found that the changes in synaptic transmission in striatal MSNs in parkinsonian and dyskinetic mice correlate with changes in spine morphology, rather than with changes in spine density. In particular, we show that in D1-MSNs, EPSP-spike coupling is enhanced despite spine loss and neck widening after dopamine depletion, whereas in dyskinesia, in addition to wider necks, mushroom spines exhibit increased volume, length, and head diameter, which might compensate for spine loss. In contrast, in D2-MSNs, dopamine depletion produces spine pruning, reduces synaptic transmission and increases firing rate. Chronic L-DOPA treatment restores spine density and neuronal excitability, but not the synaptic strength, likely because newly born spines are not fully functional due to lower PSD content and thinner necks (Fig. 7). These findings provide compelling evidence that abnormal spine morphology correlates with dyskinetic behaviors.

Notes

This work was supported by grants from the Spanish Ministries de Economía y Competitividad and Sanidad y Política Social, ISCIII: SAF2013-48532-R, CIBERNED ref. CB06/05/0055 and by SECITI from Mexico ref 037-2016 to RM, and by a grant from the Junta de Comunidades de Castilla-La Mancha (PPII-2014-005-P) to RL. OS is funded by CONACYT and SECITI (Mexico) for scholarship The authors would like to thank Mrs. Emilia Rubio and Mrs. Beatriz Pro for their excellent technical assistance and Dr. J. DeFelipe for providing the Lucifer-Yellow antibody. *Conflict of interest statement*: The authors declare that they have no conflicts of interest.

References

Albin RL, Young AB, Penney JB. 1989. The functional anatomy of basal ganglia disorders. Trends Neurosci. 12:366–375.

Andre VM, Cepeda C, Cummings DM, Jocoy EL, Fisher YE, William Yang X, Levine MS. 2010. Dopamine modulation of excitatory currents in the striatum is dictated by the expression of D1 or D2 receptors and modified by endocannabinoids. Eur J Neurosci. 31:14–28.

Azdad K, Chavez M, Don Bischop P, Wetzelaer P, Marescau B, De Deyn PP, Gall D, Schiffmann SN. 2009. Homeostatic plasticity of striatal neurons intrinsic excitability following dopamine depletion. PloS One. 4:e6908.

Bolam JP, Hanley JJ, Booth PA, Bevan MD. 2000. Synaptic organisation of the basal ganglia. J Anat. 196 (Pt 4):527–542.

Bourne JN, Harris KM. 2008. Balancing structure and function at hippocampal dendritic spines. Ann Rev Neurosci. 31:47–67.

Calabresi P, Centonze D, Bernardi G. 2000. Electrophysiology of dopamine in normal and denervated striatal neurons. Trends Neurosci. 23 (Suppl 10):S57–S63.

Calabresi P, Centonze D, Gubellini P, Marfia GA, Bernardi G. 1999. Glutamate-triggered events inducing corticostriatal long-term depression. J Neurosci. 19:6102–6110.

Calabresi P, Pisani A, Mercuri NB, Bernardi G. 1993. Heterogeneity of metabotropic glutamate receptors in the striatum: electrophysiological evidence. Eur J Neurosci. 5:1370–1377.

Darmopil S, Martin AB, De Diego IR, Ares S, Moratalla R. 2009. Genetic inactivation of dopamine D1 but not D2 receptors inhibits L-DOPA-induced dyskinesia and histone activation. Biol Psychiatry. 66:603–613.

Day M, Wang Z, Ding J, An X, Ingham CA, Shering AF, Wokosin D, Ilijic E, Sun Z, Sampson AR, Mugnaini E, Deutch AY, Sesack SR, Arbuthnott GW, Surmeier DJ. 2006. Selective elimination of glutamatergic synapses on striatopallidal neurons in Parkinson disease models. Nat Neurosci. 9:251–259.

Deutch AY, Colbran RJ, Winder DJ. 2007. Striatal plasticity and medium spiny neuron dendritic remodeling in parkinsonism. Parkinsonism Relat Disord. 13 (Suppl 3):S251–S258.

Dumitriu D, Laplant Q, Grossman YS, Dias C, Janssen WG, Russo SJ, Morrison JH, Nestler EJ. 2012. Subregional, dendritic compartment, and spine subtype specificity in cocaine regulation of dendritic spines in the nucleus accumbens. J Neurosci. 32:6957–6966.

Feyder M, Bonito-Oliva A, Fisone G. 2011. L-DOPA-induced dyskinesia and abnormal signaling in striatal medium spiny neurons: focus on dopamine D1 receptor-mediated transmission. Front Behav Neurosci. 5:71.

Fieblinger T, Graves SM, Sebel LE, Alcacer C, Plotkin JL, Gertler TS, Chan CS, Heiman M, Greengard P, Cenci MA, Surmeier DJ. 2014. Cell type-specific plasticity of striatal projection neurons in parkinsonism and L-DOPA-induced dyskinesia. Nat Comm. 5:5316.

Galarraga E, Hernandez-Lopez S, Reyes A, Barral J, Bargas J. 1997. Dopamine facilitates striatal EPSPs through an L-type Ca^{2+} conductance. Neuroreport. 8:2183–2186.

Gardoni F, Picconi B, Ghiglieri V, Polli F, Bagetta V, Bernardi G, Cattabeni F, Di Luca M, Calabresi P. 2006. A critical interaction between NR2B and MAGUK in L-DOPA induced dyskinesia. J Neurosci. 26:2914–2922.

Gerfen CR, Surmeier DJ. 2011. Modulation of striatal projection systems by dopamine. Ann Rev Neurosci. 34:441–466.

Grueter BA, Robison AJ, Neve RL, Nestler EJ, Malenka RC. 2013. ΔFosB differentially modulates nucleus accumbens direct and indirect pathway function. Proc Natl Acad Sci USA. 110 (5):1923–1928.

Harris KM, Jensen FE, Tsao B. 1992. Three-dimensional structure of dendritic spines and synapses in rat hippocampus (CA1) at postnatal day 15 and adult ages: implications for the maturation of synaptic physiology and long-term potentiation. J Neurosci. 12:2685–2705.

Hernandez-Flores T, Hernandez-Gonzalez O, Perez-Ramirez M B, Lara-Gonzalez E, Arias-Garcia MA, Duhne M, Perez-Burgos A, Prieto GA, et al. 2015. Modulation of direct pathway striatal projection neurons by muscarinic M(4)-type receptors. Neuropharmacol. 89:232–244.

Ingham CA, Hood SH, Arbuthnott GW. 1989. Spine density on neostriatal neurones changes with 6-hydroxydopamine lesions and with age. Brain Res. 503:334–338.

Jenner P. 2008. Molecular mechanisms of L-DOPA-induced dyskinesia. Nat Rev Neurosci. 9:665–677.

Kawaguchi Y. 1997. Neostriatal cell subtypes and their functional roles. Neurosci Res. 27:1–8.

Lazcano Z, Solis O, Díaz A, Brambila E, Aguilar-Alonso P, Guevara J, Flores G. 2015. Dendritic morphology changes in neurons from the ventral hippocampus, amygdala and nucleus accumbens in rats with neonatal lesions into the prefrontal cortex. Synapse. 69(6):314–25.

Lujan R, Nusser Z, Roberts JD, Shigemoto R, Somogyi P. 1996. Perisynaptic location of metabotropic glutamate receptors mGluR1 and mGluR5 on dendrites and dendritic spines in the rat hippocampus. Eur J Neurosci. 8:1488–1500.

McNeill TH, Brown SA, Rafols JA, Shoulson I. 1988. Atrophy of medium spiny I striatal dendrites in advanced Parkinson's disease. Brain Res. 455:148–152.

Murer MG, Moratalla R. 2011. Striatal signaling in L-DOPA-induced dyskinesia: common mechanisms with drug abuse and long term memory involving D1 dopamine receptor stimulation. Front Neuroanat. 5:51.

Parker PR, Lalive AL, Kreitzer AC. 2016. Pathway-specific remodeling of thalamostriatal synapses in parkinsonian mice. Neuron. 89(4):734–740.

Pavon N, Martin AB, Mendialdua A, Moratalla R. 2006. ERK phosphorylation and FosB expression are associated with L-DOPA-induced dyskinesia in hemiparkinsonian mice. Biol Psychiatry. 59:64–74.

Perez-Ortega J, Duhne M, Lara-Gonzalez E, Plata V, Gasca D, Galarraga E, Hernandez-Cruz A, Bargas J. 2016. Pathophysiological signatures of functional connectomics in parkinsonian and dyskinetic striatal microcircuits. Neurobiol Dis. doi:10.1016/j.nbd.2016.02.023.

Plata V, Duhne M, Pérez-Ortega J, Hernández-Martinez R, Rueda-Orozco P, Galarraga E, Drucker-Colín R, Bargas J. 2013. Global actions of nicotine on the striatal microcircuit. Front Syst Neurosci. 6(7):78.

Porras G, Berthet A, Dehay B, Li Q, Ladepeche L, Normand E, Dovero S, Martinez A, Doudnikoff E, Martin-Negrier ML, Chuan Q, Bloch B, Choquet D, Boue-Grabot E, Groc L, Bezard E. 2012. PSD-95 expression controls L-DOPA dyskinesia through dopamine D1 receptor trafficking. J Neurosci. 122:3977–3989.

Robinson TE, Kolb B. 2004. Structural plasticity associated with exposure to drugs of abuse. Neuropharmacology. 47(Suppl 1): 33–46.

Rodriguez A, Ehlenberger DB, Dickstein DL, Hof PR, Wearne SL. 2008. Automated three-dimensional detection and shape classification of dendritic spines from fluorescence microscopy images. PLoS One. 3:e1997.

Ruiz-DeDiego I, Mellstrom B, Vallejo M, Naranjo JR, Moratalla R. 2015. Activation of DREAM (downstream regulatory element antagonistic modulator), a calcium-binding protein, reduces L-DOPA-induced dyskinesias in mice. Biol Psychiatry. 77: 95–105.

Santini E, Valjent E, Usiello A, Carta M, Borgkvist A, Girault JA, et al. 2007. Critical involvement of cAMP/DARPP-32 and extracellular signal-regulated protein kinase signaling in L-DOPA-induced dyskinesia. J Neurosci. 27:6995–7005.

Solis O, Espadas I, Del-Bel EA, Moratalla R. 2015a. Nitric oxide synthase inhibition decreases l-DOPA-induced dyskinesia and the expression of striatal molecular markers in Pitx3(-/-) aphakia mice. Neurobiol Dis. 73:49–59.

Solís O, Garcia-Montes JR, González-Granillo A, Xu M, Moratalla R. 2015b. Dopamine D3 receptor modulates L-DOPA-induced dyskinesia by targeting D1 receptor-mediated striatal signaling. Cereb Cortex. doi:10.1093/cercor/bhv231.

Solis O, Limón DI, Flores-Hernández J, Flores G. 2007. Alterations in dendritic morphology of the prefrontal cortical and striatum neurons in the unilateral 6-OHDA-rat model of Parkinson's disease. Synapse. 61:450–458.

Stephens B, Mueller AJ, Shering AF, Hood SH, Taggart P, Arbuthnott GW, Bell JE, Kilford L, Kingsbury AE, Daniel SE, Ingham CA. 2005. Evidence of a breakdown of corticostriatal connections in Parkinson's disease. Neuroscience. 132: 741–754.

Stuart G, Spruston N, Sakmann B, Häusser M. 1997. Action potential initiation and backpropagation in neurons of the mammalian CNS. Trends Neurosci. 20 (3):125–131.

Suarez LM, Solis O, Carames JM, Taravini IR, Solis JM, Murer MG, Moratalla R. 2014. L-DOPA treatment selectively restores spine density in dopamine receptor D2-expressing projection neurons in dyskinetic mice. Biol Psychiatry. 75:711–722.

Surmeier DJ, Bargas J, Hemmings HCJr, Nairn AC, Greengard P. 1995. Modulation of calcium currents by a D1 dopaminergic protein kinase/phosphatase cascade in rat neostriatal neurons. Neuron. 14:385–397.

Toy WA, Petzinger GM, Leyshon BJ, Akopian GK, Walsh JP, Hoffman M V, Vučković MG, Jakowec MW. 2014. Treadmill exercise reverses dendritic spine loss in direct and indirect striatal medium spiny neurons in the 1-methyl-4-phenyl-1,2,3,6-tetrahydropyridine (MPTP) mouse model of Parkinson's disease. Neurobiol Dis. 63:201–209.

Usowicz MM, Sugimori M, Cherksey B, Llinas R. 1992. P-type calcium channels in the somata and dendrites of adult cerebellar Purkinje cells. Neuron. 9:1185–99.

Villalba R M, Wichmann T, Smith Y. 2014. Neuronal loss in the caudal intralaminar thalamic nuclei in a primate model of Parkinson's disease. Brain Struct Funct. 219:381–394.

Villalba RM, Lee H, Smith Y. 2009. Dopaminergic denervation and spine loss in the striatum of MPTP-treated monkeys. Exp Neurol. 215:220–227.

Westenbroek RE, Hell JW, Warner C, Dubel SJ, Snutch TP, Catterall WA. 1992. Biochemical properties and subcellular distribution of an N-type calcium channel alpha 1 subunit. Neuron. 9:1099–1115.

Yuste R, Bonhoeffer T. 2004. Genesis of dendritic spines: insights from ultrastructural and imaging studies. Nat Rev Neurosci. 5:24–34.

Zaja-Milatovic S, Milatovic D, Schantz AM, Zhang J, Montine KS, Samii A, Deutch AY, Montine TJ. 2005. Dendritic degeneration in neostriatal medium spiny neurons in Parkinson disease. Neurology. 64:545–547.

Zhang Y, Meredith GE, Mendoza-Elias N, Rademacher DJ, Tseng KY, Steece-Collier K. 2013. Aberrant restoration of spines and their synapses in L-DOPA-induced dyskinesia: involvement of corticostriatal but not thalamostriatal synapses. J Neurosci. 33:11655–11667.